On localized solutions of an equation governing Benard–Marangoni convection

Christo I. Christov*

Instituto Nacional de Meteorologia, Ciudad Universitaria, Madrid, Spain

Manuel G. Velarde

Facultad de Ciencias, Universidad Nacional de Educación a Distancia, Madrid, Spain

Provided here is numerical evidence of localized solutions, solitary waves, in a model equation for Bénard convection driven by interfacial stresses (Marangoni effect).

Keywords: Kuramoto–Sivashinsky–Velarde equation, interfacial instability, Benard convection, surface tension-driven convection, variational imbedding

Introduction

Bénard–Marangoni convection refers to the thermocapillary flow developing in a shallow horizontal liquid layer heated from below when its upper boundary is a free surface open to the ambient air.[1–4] In the simplified case of a two-dimensional geometry the thermoconvective evolution of the open surface can be described by the following equation

$$\frac{\partial u}{\partial t} + \gamma\left(\frac{\partial u}{\partial x}\right)^2 + \delta\frac{\partial}{\partial x}\left(u\frac{\partial u}{\partial x}\right) + \frac{\partial^2 u}{\partial x^2} + \frac{\partial^4 u}{\partial x^4} + \beta u - \frac{\gamma}{L}\int_0^L \left(\frac{\partial u}{\partial x}\right)^2 dx = 0 \quad (1)$$

where thermocapillary and buoyancy effects are taken into account.[5,6] Equation (1), arising in Bénard–Marangoni convection, is a variation on the Kuramoto–Sivashinsky (KS) equation[3,6,7]

$$\frac{\partial u}{\partial t} + u\frac{\partial u}{\partial x} + \frac{\partial^2 u}{\partial x^2} + \frac{\partial^4 u}{\partial x^4} = 0 \quad (2)$$

where for simplicity we have equated all coefficients to unity. Note in equation (1) the additional nonlinear term $\delta(uu_x)_x$. In addition, the coefficient δ in equation (1) can change sign according to the *effective* gravity level, and thus equation (1) accounts for both ground and space (microgravity) conditions. When $\delta < 0$ (negative) such a term plays a stabilizing role whereas if $\delta > 0$ (positive) it tends to destabilize the surface.[5]

In the past few years a number of generalizations of the KS equation have been published in the literature. For instance the KS equation has been supplemented with a term containing the third derivative in space thus accounting for inertia and *dispersion* effects, which amounts to a combination of the KS equation with the Korteweg–de Vries equation (KdV).[8] In Ref. 8 the authors show how profoundly the addition of the third derivative affects the KS equation, generally leading to standard KdV solitary waves even when the order of magnitude of the third derivative is of the order of the values of the coefficients of the remaining terms. Here, on the contrary, we are interested in a generalization of the KS equation when the energy supply provided by the Marangoni effect and the dissipation, i.e., when the second and fourth derivatives and the nonlinearity controlled by δ in equation (1) dominate while dispersion is negligible and yet localized excitations, steady or otherwise, appear.

The role of the new nonlinear term in equation (1) (KSV hereafter) was illustrated in Ref. 6 by means of direct numerical simulations, and it was shown that if the eikonal nonlinearity term u_x^2 is removed ($\gamma = 0, \beta \geq 0$) then the solution of (1) blows up in finite time. Otherwise the chaotic dynamics of equation (1) are essentially the same as for the KS equation.[7] Note that the KSV–KdV equation has been recently derived.[9] On the other hand note also that the same nonlinearity was earlier found in a different context.[10] However, as in the equation derived in Ref. 10 there is no fourth-order derivative in space; though it shares the same

* Permanent address: Institute of Meteorology and Hydrology, Bulgarian Academy of Sciences, Sofia 1184, Bulgaria.
Address reprint requests to Prof. Velarde at Instituto Pluridisciplinar, Universidad Complutense, Paseo Juan XXIII, No. 1, Madrid 28.040, Spain.

Received 6 February 1992; revised 22 July 1992; accepted 25 September 1992

nonlinearity with equation (1) its mathematical properties are *qualitatively* different.

We concentrate our attention on the *localized* solutions of equation (1) in the form of one-dimensional traveling waves. As the eikonal nonlinearity term is essential and cannot be removed, then $\gamma \neq 0$. With no other reason we set $\gamma = 3$ for the sake of definiteness. Our main purpose is to assess the role played by the nonlinear term $\delta(uu_x)_x$ in the shape formation of a *solitary* wave. To simplify the picture we neglect the linear resistance term βu, i.e., we take $\beta = 0$. The intricate interplay between the nonlinearities and the linear resistance would require special care, and this shall be done elsewhere.

The *localized* solutions of (1) can be either *homoclinics* when $u \to 0$ for $x \to +\infty$ or $-\infty$ (the traditional *solitary* wave in the form of a localized hump decaying at both infinitely far sides) or *heteroclinics* (a *kink*) when $u \to u_{-\infty}$ for $x \to -\infty$ and $u \to u_{+\infty}$ for $x \to +\infty$. The second case is more general, and we shall concern ourselves in what follows with the heteroclinics of (1). It is clear that the derivative u_x of a localized solution is always a *homoclinics* and hence the integral term in (1) has a finite value even when $L \to \infty$. Then taking $L \to \infty$ we can neglect that term in equation (1) and consider a simplified version of (1), namely

$$\frac{\partial u}{\partial t} + \gamma\left(\frac{\partial u}{\partial x}\right)^2 + \delta\frac{\partial}{\partial x}\left(u\frac{\partial u}{\partial x}\right) + \frac{\partial^2 u}{\partial x^2} + \frac{\partial^4 u}{\partial x^4} = 0 \qquad (3)$$

Consider traveling waves that are functions only of the coordinate

$$\xi = x\text{-}ct \qquad (4)$$

when (3) reduces to the following ODE, $u = u(\xi)$,

$$-cu' + (\gamma + \delta)u'^2 + \delta uu'' + u'' + u^{IV} = 0 \qquad (5)$$

Here c is the *phase velocity* or *celerity* of the traveling wave and a "prime" denotes derivative with respect to ξ (superscript prime number indicates order of derivative).

When $\delta = 0$ (KS case) using the transformation

$$v = u' \quad \text{or} \quad u = \int_{-\infty}^{\xi} v(\xi_1)\,d\xi_1 + u_{-\infty} \qquad (6)$$

it permits lowering of the order of (5) from fourth order in "u" to third order in "v". Unfortunately, it is not the case when the full equation (5) with $\delta \neq 0$ is considered. Still we prefer to use the substitution (6) because it reduces the number of computer operations when implementing the numerical algorithm. So, we recast (5) to

$$-cv + (\gamma + \delta)v^2 + \delta uv' + v''' = 0 \qquad (7)$$

where u is defined by the second equation in (6). Of course, the substitution (6) is formally equivalent to integration and $u_{-\infty}$ is in fact an integration constant. Appearance of a new constant $u_{-\infty}$ immediately increases in order of magnitude the number of numerical "experiments" to be performed. One may argue that equation (1) is for the deviation from the main state and hence at infinity "u" should decay to zero. It is not clear, however, at which infinity ($-\infty$ or $+\infty$) the function u decays for this depends on the specific physical case considered. So we should allow the more general case $u_{-\infty} \neq 0$. Fortunately, under some not very restrictive limitations in the relationship between δ and $u_{-\infty}$ one can introduce an appropriate scaling and exclude $u_{-\infty}$ from the equation. Indeed, upon introducing (6) into (7) we get

$$-cv + (\gamma + \delta)v^2 + \delta\left(\int_{-\infty}^{\xi} v(\xi)\,d\xi\right)v + (1 + \delta u_{-\infty})v' + v''' = 0 \qquad (8)$$

Let us call v_0 the function that satisfies (7) when $u_{-\infty} = 0$. Then rescaling again the quantities

$$v = (1 + \delta u_{-\infty})^{3/2} v_0(\xi\sqrt{1 + \delta u_{-\infty}}), \qquad c_1 = c(1 + \delta u_{-\infty})^{-3/2} \qquad (9)$$

we get

$$-c_1 v_0 + (\gamma + \delta)v_0^2 + \delta\left(\int_{-\infty}^{\xi} v_0(\xi)\,d\xi\right)v_0' + v_0' + v'''_0 = 0 \qquad (10)$$

Naturally, the scaling (8) demands that

$$\begin{aligned} &u_{-\infty} > -\frac{1}{\delta} && \text{for } \delta > 0 \\ &u_{-\infty} < \frac{1}{|\delta|} && \text{for } \delta < 0 \\ &-\infty < u_{-\infty} < +\infty && \text{for } \delta = 0 \end{aligned} \qquad (11)$$

Hence we shall consider only the solitary waves of the kink type with $u_{-\infty}$ satisfying conditions (11).

Putting (10) as a system of ODEs in normal form we have (for simplicity denote now $x \equiv v_0$)

$$\begin{aligned} &x' - y = 0 \\ &y' - z = 0 \\ &z' + y[1 + \delta u(\xi)] + (\gamma + \delta)x^2 - cx = 0, \\ &u \equiv \int_{-\infty}^{\xi} x(\xi)\,d\xi \end{aligned} \qquad (12)$$

for which the inverse boundary value problem

$$x, y, z \to 0 \quad \text{for } \xi \to \pm\infty \qquad (13)$$

is to be solved if localized solutions are sought.

Variational imbedding[11,12]

In the previous section we arrived at the inverse problem of identifying the homoclinic trajectory of (12). The problem is of inverse nature because we have two boundary conditions for each unknown function x, y, z, while the corresponding equation is of first order.

The straightforward approach to calculating the homoclinics is to use the so-called shooting procedure, which consists in solving the initial value problem for (12) with $x = y = 0$ and $z = \epsilon_0$ at the left boundary of the (reduced) interval $\xi = \xi_{-\infty}$. This must be carried out many times with different values of ϵ_0 until the value for ϵ_0 is found for which the boundary conditions at the right boundary of the interval, namely, $\xi = \xi_{+\infty}$ are also satisfied. For the problem under consideration the shooting procedure was being applied, e.g., in Refs. 13 and 14 (in Ref. 13 to an even more complicated equation). The difficulty with shooting techniques is that the initial value problem for equation (12) is intrinsically highly unstable, and therefore the requirements on mesh size and other properties of the difference scheme are very stringent.[14]

Recently[11] a different approach to the inverse problems was proposed. It is a variational imbedding procedure (MVI hereafter) and was originally implemented for calculating the shape of homoclinics of the Lorenz system. The essence of the new method is in the replacement of the original unstable initial-value problem by the problem of minimization of the quadratic functional of the equations of the governing system

$$J = \int_{-\infty}^{\infty} \{(x' - y)^2 + (y' - z)^2 + [z' + y + \delta uy + (\gamma + \delta)x^2 - cx]^2\}\, d\xi \quad (14)$$

Here we shall use a MVI that is slightly modified with respect to that used in Refs. 11 and 12, namely we discretize the problem yet on the level of the functional; i.e., J is approximated by the function of many variables

$$I = \sum_{i=2}^{N-1} \left\{ \left(\frac{x_{i+1} - x_i}{h} - y_i \right)^2 + \left(\frac{y_{i+1} - y_i}{h} - z_i \right)^2 + \left[\frac{z_{i+1} - z_i}{h} + (\gamma + \delta)x_i^2 - cx_i + (1 + \delta u_i)y_i \right]^2 \right\} \quad (15)$$

This permits us to derive the difference scheme in *conservative* form. The scheme provides only a first-order spatial approximation $0(h)$ of the functional, but it is enough for the purpose here because the higher order approximations require a further increase in the number of arithmetic computations per grid point.

The necessary conditions for minimization of the function of many variables, I, is to have all its partial derivatives with respect to different arguments equal to zero, namely

$$\frac{\partial I}{\partial x_i} = 0, \frac{\partial I}{\partial y_i} = 0, \frac{\partial I}{\partial z_i} = 0, \quad i = 2, \ldots, N - 1 \quad (16)$$

Differentiation with respect to x_1, y_1, z_1, x_N, y_N, z_N is not performed because these are specified by the boundary conditions, namely

$$x_1 = y_1 = z_1 = x_N = y_N = z_N = 0 \quad (17)$$

Then, the different derivatives in (15) give the three main groups of difference equations

$$\frac{x_{i+1} - 2x_i + x_{i-1}}{h^2} - [2(\gamma + \delta)^2 x_i^2 + c^2]x_i = -3(\gamma + c)cx_i^2 + \frac{y_i - y_{i-1}}{h} + [2(\gamma + \delta)x_i - c]\left[\frac{z_{i+1} - z_i}{h} + (1 + \delta u_i)y_i \right] \quad (18\text{-x})$$

$$\frac{y_{i+1} - 2y_i + y_{i-1}}{h^2} - [1 + (1 + \delta u_i)^2]y_i = \frac{z_i - z_{i-1}}{h} - \frac{x_{i+1} - x_i}{h} + \left[\frac{z_{i+1} - z_i}{h} + (\gamma + \delta)x_i^2 - cx_i \right](1 + \delta u_i) \quad (18\text{-y})$$

$$\frac{z_{i+1} - 2z_i + z_{i-1}}{h^2} - z_i = -\frac{y_{i+1} - y_i}{h} + \frac{1}{h}\{[(\gamma + \delta)x_i^2 + (1 + \delta u_i)y_i - cx_i] - [(\gamma + \delta)x_{i-1}^2 + (1 + \delta u_{i-1})y_{i-1} - cx_{i-1}]\} \quad (18\text{-z})$$

The way we posed the system (18) yields clues on how to linearize it and how to carry out the iterations. For example, the first equation can be treated iteratively as follows

$$\frac{1}{h^2}[x_{i+1}^{n+1} - 2x_i^{n+1} + x_{i-1}^{n+1}] - [2(\gamma + \delta)^2 (x_i^n)^2 + c^2]x_i^{n+1} = -3(\gamma + c)c(x_i^n)^2 + \frac{y_i^n - y_{i-1}^n}{h} + [2(\gamma + \delta)x_i^n - c]\left[\frac{z_{i+1}^n - z_i^n}{h} + (1 + \delta u_i^n)y_i^n \right] \quad (19)$$

i.e., only the main terms are taken on the new iterative stage, the latter being distinguished by the superscript "$(n + 1)$". This is attractive because we arrive at a three-diagonal linear system with strongly dominating principal diagonal.

In fact we actually did implement the scheme (19) and at the beginning of the iterations the convergence was very fast, but as the solution was approached the pace became so slow that the advantage was lost.

The most consistent approach to improve the con-

vergence is to use Newton's quasilinearization. Unfortunately, in our case using Newton's method yields a conjugate tridiagonal system for the vector (x_i, y_i, z_i), which poses problems with the computational implementation. Of course these difficulties can be overcome but once again at the expense of increasing the number of arithmetic operations per unit mesh point. A reasonable compromise can be obtained by the separate linearization of (15).

Consider the $(n + 1)st$ iterative stage. Suppose we are initially dealing with x. Then we consider the $(n + \frac{1}{3})th$ iteration for the functional I, namely

$$I^{n+1/3} = \sum_{i=2}^{N-1} \left\{ \left(\frac{x_{i+1}^{n+1} - x_i^{n+1}}{h} - y_i^n \right)^2 + \left(\frac{y_{i+1}^n - y_i^n}{h} - z_i^n \right)^2 \cdot \left[\frac{z_{i+1}^n - z_i^n}{h} + 2(\gamma + c)x_i^n x_i^{n+1} - c x_i^{n+1} + (1 + \delta u_i^n) y_i^n - (\gamma + c)x_i^{n^2} \right] \right\} \quad (20\text{-x})$$

i.e., we quasilinearize just the term containing the nonlinear contribution from the first unknown. Then the first difference system for the set function x_i reads

$$\frac{1}{h^2}(x_{i+1}^{n+1} - 2x_i^{n+1} + x_{i-1}^{n+1}) - [2(\gamma + c)x_i^n - c]^2 x_i^{n+1} = \frac{y_i - y_{i-1}}{h} + [2(\gamma + \delta)x_i^n - c]\left[\frac{z_{i+1}^n - z_i^n}{h} + (1 + \delta u_i^n) y_i^n - (\gamma + \delta)x_i^{n^2} \right] \quad (21\text{-x})$$

At first sight (21) does not differ significantly from (19). In the limit $n \to \infty$, i.e., when $|x^{n+1} - x^n| \to 0$ the two equations give in fact the difference approximation $(18 - x)$. However, although small, the differences between (21) and (19) cannot be overlooked, and the iterations conducted using (21-x) exhibit linear but stable convergence with increasing n.

The problem with the other two functions is much less complicated because there are no nonlinear terms involving y and z (the system is bilinear with respect to y and z). So the next "fractional-step" iteration of the functional is

$$I^{n+2/3} = \sum_{i=2}^{\infty} \left\{ \left(\frac{x_{i+1}^{n+1} - x_i^{n+1}}{h} - y_i^{n+1} \right)^2 + \left(\frac{y_{i+1}^{n+1} - y_i^{n+1}}{h} - z_i^n \right)^2 + \left[\frac{z_{i+1}^n - z_i^n}{h} + (\gamma + c)(x_i^{n+1})^2 - c x_i^{n+1} + (1 + \delta u_i^{n+1}) y_i^{n+1} \right]^2 \right\} \quad (20\text{-y})$$

Here x_i^{n+1} is already known from the $(n + \frac{1}{3})th$ step. Correspondingly, u_i^{n+1} is calculated from x_i^{n+1} by means of the trapezoidal rule. Then the system of equations for the minimization of $I^{n+2/3}$ with respect to the unknowns y_i^{n+1} is the following

$$\frac{1}{h^2}(y_{i+1}^{n+1} - 2y_i^{n+1} + y_{i-1}^{n+1}) - [(1 + \delta u_i^{n+1})^2 + 1] y_i^{n+1} = \frac{z_i^n - z_{i-1}^n}{h} - \frac{x_{i+1}^{n+1} - x_i^{n+1}}{h} + \left[\frac{z_{i+1}^{n+1} - z_i^{n+1}}{h} + (\gamma + \delta)(x_i^{n+1})^2 - c x_i^{n+1} \right](1 + \delta u_i^{n+1}) \quad (21\text{-y})$$

This is once more a linear three-diagonal difference system.

In the same manner we treat the minimization with respect to z, namely, the third fractional iterative step for the functional

$$I^{n+1} = \sum_{i=2}^{\infty} \left\{ \left(\frac{x_{i+1}^{n+1} - x_i^n}{h} - y_i^{n+1} \right)^2 + \left(\frac{y_{i+1}^{n+1} - y_i^{n+1}}{h} - z_i^{n+1} \right) + \left[\frac{z_{i+1}^{n+1} - z_i^{n+1}}{h} + (\gamma + c)(x_i^{n+1})^2 - c x_i^{n+1} + (1 + \delta u_i^{n+1}) y_i^{n+1} \right]^2 \right\} \quad (21\text{-z})$$

The corresponding system of linear equations is

$$\frac{1}{h^2}(z_{i+1}^{n+1} - 2z_i^{n+1} + z_{i-1}^{n+1}) - z_i^{n+1} = -\frac{y_{i+1}^{n+1} - y_i^{n+1}}{h} + \frac{1}{h}[(\gamma + \delta)(x_i^{n+1})^2 - cx_i^{n+1} + (1 + \delta u_i^{n+1})y_i^{n+1}]$$

$$+ \frac{1}{h}[(\gamma + \delta)(x_{i-1}^{n+1})^2 - cx_{i-1}^{n+1} + (1 + \delta u_{i-1}^{n+1})y_{i-1}^{n+1}] \quad (21\text{-}z)$$

Thus we have a complete system of difference equations for the set functions we are looking for. Equations (21) are to be satisfied at all points starting from $i = 2$ to $i = N - 1$ while at the boundary points the boundary conditions (17) are imposed.

Here becomes apparent the advantage of using the substitution (6) that for the set functions has the form

$$u^{n+1} = \int_{-\infty}^{x} x^{n+1}(\xi)\, d\xi$$

Otherwise we would be faced with four equations of type (21) and the computational time required would be about 30% greater, inasmuch as solving the three-diagonal system requires order of magnitude more calculations than the simple trapezoidal rule, i.e., the total amount of computations is defined by the number of main equations. In our case these are (21).

Iterations are conducted until

$$\max\{(x_i^{n+1} - x_i^n), (y^{n+1} - y^n), (z^{n+1} - z^n)\} < \epsilon$$
$$\epsilon = 10^{-7}$$

Computations are made using double precision.

Here the major advantage of the MVI becomes apparent. Even if we are not "on" the exact "location" c^* of the nonlinear eigenvalue problem we can still obtain a solution to the variational imbedding problem that is fairly close to the shape of the real one, and we can define the optimal parameters of the mesh for a given c. Then we proceed to improve the accuracy in c. For illustration we start with $\gamma = 3$, $\delta = 0$, $c = 1$. Let us see the main difficulties to be overcome.

Verification of the difference scheme

Let us denote by N the total number of grid points. It cannot be very large (although it is desired) due to computer limitations. It cannot be very small either because then the mesh would not be dense enough to allow sufficient flexibility. So we choose $N = 1601$ to start with. The role of N is discussed in detail below.

Another important integer parameter is the number NS at which the origin of the coordinate system is placed. For different values of control parameters (γ, δ) and celerity c, the optimal value of NS may vary significantly, and this will be shown in the next section. For the test case under consideration it can be shown from the linearized equation that the solitary wave of homoclinics type (if it exists at all) decays twice faster at $-\infty$ than at $+\infty$. So the proper position for the origin of the coordinate system is approximately $\frac{1}{3}$ of the interval under consideration. As far as in the right-hand part of the interval the forerunner is governed by the wavy decaying solution we can still further increase the portion allotted to it and set $NS = 5N/16$ (a bit less than $\frac{1}{3}$).

Role of the initial conditions

Having N and NS specified, one can construct an initial condition. As it appears from the numerical experiments the exact form of the initial condition is not especially important. Rather, the most important item is the amplitude of the initial condition. So we simply set

$$\left.\begin{aligned} u_i &= C_{inl}(i - 1)(NS - i)/NS \\ u_{NS+i} &= -u_{NS-i} \end{aligned}\right\} \text{for } i \leq NS$$
$$u_{2NS+j} = 0 \qquad j = 1, \ldots, N - 2NS \quad (22)$$

In case $2NS > N$ the construction is the same but instead of NS $NS_1 = N - NS$ is used.

The constant C_{inl} defines the amplitude of the initial condition. It is an important quantity as we are faced with a bifurcation problem in which the trivial solution is always present. If we choose a small value (e.g., $C_{inl} < 1$) then the iterations converge to the trivial solution. If we select a very large $C_{inl} > 100$ then for certain cases the iterations may diverge. It turns out that $C_{inl} \approx 10$ is a suitable choice for the amplitude of the initial condition.

The actual infinity

Further we have the problem of selecting the most sensitive parameter, i.e., the finite size of the interval L. If the selected value is too small the problems of the previous abset are exaggerated. Either the solution rapidly converges to zero or it diverges. Going to larger L eliminates this difficulty but a new one develops. For very large L two localized structures can appear in the interval under consideration that are the kind of bound states discussed in Ref. 8. Here it should be mentioned that we keep $N = 1601$, $c = 1$ while playing with L.

When we tried a smaller value $L = 10$ an instability of the iterative process occurred. Rather than overcoming it by some standard techniques (e.g., relaxation) we took a larger value, namely, $L = 20$. For the latter a nontrivial solution to the imbedding problem was found after about 80 iterations, and it gave $6 \cdot 10^{-5}$ for I. This result means that we are probably very close to the solution sought. So, starting with it as an initial condition we increase L to 32 and after less than 30 iterations, the solution is substantially improved in detail though generally retaining the same shape.

Moreover, the minimum value is drastically reduced down to $1.6 \cdot 10^{-6}$. The next increase is to 40 where the minimum falls to $1.2 \cdot 10^{-6}$ (remember that starting directly with $L = 40$ leads to a two-hump solution of type of bound state). Further increase of L with the same number of points ($N = 1601$) gives a slight increase of the minimum of I and finally when moving from $L = 80$ to $L = 100$ the solution decays to zero in the course of iterations. These effects are connected with the fact that the mesh becomes too rough. So, for the case under consideration with $\gamma = 3$, $c = 1$ we can say that the optimal value of L is 40. To implement the above described "chase" we used a spline interpolation method[15] to recalculate the shape of the initial condition over the new set of grid points when the value of L is increased (decreased) with fixed number of points, N. Generally, the procedure allows us to change all mesh parameters: N, NS, and L (or h) simultaneously as we illustrate in the following subsection.

The influence of the mesh resolution (number of grid points N)

Taking advantage of the spline approximation procedure we were able to change the number of grid points with fixed L and fixed ratio $(NS - 1)/(N - 1) = \frac{5}{16}$. In all cases to reduce the number of calculations we started from the calculated in the previous subsection shape ($N = 1601$, $NS = 501$, $L = 40$). These calculations illustrated the convergence of the difference solution to the solution of the differential problem. It turned out that in the main portion of the interval $[-12, +16]$ where the predominant part of the energy of the solitary wave is concentrated (about 99.9%) the solutions with $N = 1601$, 3201, and 6401 virtually coincide with each other and only $N = 401$ (respectively, $N = 801$) differs up to 5% (respectively, 2%) from $N = 6401$. This is a superb performance for a scheme of first-order approximation $0(h)$ with respect to the spatial discretization. Yet as far as the shape of the solitary wave solution is concerned one can fully rely on the mesh $N = 1601$.

Good agreement is observed in the far-distant portion of the interval [16, 25] where only the roughest solution $N = 401$ deviates significantly, while $N = 1601$ and higher N are fully acceptable. One must bear in mind that the actual solution is so small in that region that some of the deviation may be due to eventual round-off errors in the computer representation of the numbers.

To conclude this section we can say that the difference scheme developed here provides a good and rapidly converging approximation to the variational imbedding problem and hence we can proceed further with the essence of the imbedding.

Outline of the minimization procedure for selecting the solution of the original problem among the solutions of the MVI problem

In essence, the attractive part of the MVI procedure is that one can calculate the solution of the embedding system for values of c for which a homoclinic solution for the original system may not exist and to define thus the function $f(c) = \min_{x,y,z} I[x(\xi), y(\xi), z(\xi); c]$ for each c. Finding the minimum of this function of c is the next step, and if this minimum is equal to zero then the original problem is solved. If the minimum is far from the numerical approximation of the zero, then the conclusion is that no homoclinic solution to the original problem exists. In the present section we give a brief outline of the minimization algorithm, as a follow-up to the method developed in Ref. 11.

For a prescribed set of values of the governing parameters γ and δ the scheme is as follows: (a) It is roughly estimated the interval in which appears the local minimum of functional I as a function of c (namely, the function $f(c)$).

Usually this is done by performing an extensive set of calculations with different c. To minimize the computational costs the search is conducted in the vicinity of the c^*, which has previously been obtained for the closest set of parameters γ, δ.

(b) A procedure implementing the method of golden section is executed to locate the minimum with a priori prescribed accuracy (as a rule we set that accuracy to 2ϵ, where ϵ is the accuracy at with which the iterations for x, y, z are terminated).

In *Figure 1* we give the results of the minimization procedure with different mesh sizes. To clearly see the behavior in the vicinity of the actual minimum only six to eight of the smallest values of the functional are shown. *Table 1* provides the corresponding final result. Here the only significant shortcoming of the first-order spatial approximation of the difference scheme appears: the convergence of c to the one which is defined by the differential problem is also linear. A simple linear extrapolation gives a projection for $c \approx 1.216$ which, surprisingly enough, coincides up to the four secure digits with the result of Ref. 16. This excellent agreement gives confidence in the results of both methods, that of Ref. 16 and the present method. However, here one has some advantages in generality (see Refs.

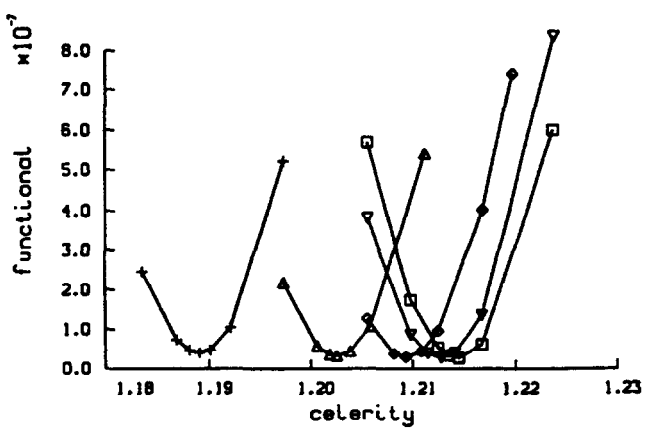

Figure 1. Accuracy of the minimization procedure of the variational functional for $c = 1$ and different mesh sizes N: + $N = 801$; △ $N = 1601$; ▽ $N = 3201$; □ $N = 6401$.

Table 1. The minimum of the functional for different meshes.

N	401	801	1601	3201	6401	∞*
c	1.1890387	1.2025537	1.2093515	1.2127570	1.2144646	1.216179
min $f(c)$	$14.1697.10^{-8}$	$6.2783.10^{-8}$	$4.0612.10^{-8}$	$3.3099.10^{-8}$	$2.9256.10^{-8}$	

* Projected by a linear Richardson extrapolation from the cases $N = 3201$ and $N = 6401$.

11, 15, and 17), and the method can be applied without any modifications to other solitary wave problems whereas the spectral technique of Ref. 16 heavily relies on some particular properties of the specific KS equation and cannot be extended to the equation considered in the present paper.

Finally, in *Figure 2* we present the solitary wave as obtained for the original problem for different mesh sizes. It is once again seen that the homoclinics shape is much less sensitive to the mesh size than the eigenvalue c for which the respective shape does exist.

To us the results of the present section suffice to show that a solitary wave does exist, and its shape is represented rather accurately by the solution $N = 6401$ given in *Figure 2*.

Before going further we mention that having the solution of a multitude of meshes with different spacings provides us with the opportunity to calculate the shape with second order $O(h^2)$ in space. The latter can be done by means of the so-called Richardson extrapolation. Let us denote by Φ_i^h the values of one of the set functions x, y, z, u obtained with given value h of the spacing. Let $\Phi_i^{h/2}$ stand for the values in the same points (the index "i") of the same function but calculated with spacing $h/2$. Then

$$\Phi_i = 2\Phi_i^{h/2} - \Phi_i^h = \Phi(x) + O(h^2) \tag{23}$$

provides a second-order approximation to $\Phi(x)$. Respectively,

$$c = 2c^{h/2} - c^h \tag{24}$$

is the "refined" value of the celerity.

To check the performance of the scheme we applied the Richardson extrapolation twice. First, from $N = 1601$ to $N = 3201$ obtaining the second-order solution on the mesh $N = 1601$ and, second, from $N = 3201$ to $N = 6401$ obtaining the said solution on the finer mesh $N = 3201$. The comparison between the two second-order solutions was perfect, less than 0.3% at the time when the maximum of the solution was of order 0.5. The accuracy of the extrapolation for c was better than 0.5%. The "ultimate" value of c is provided in *Table 1*. It has already been noted that the first four digits of our result coincide exactly with the value reported in Ref. 16.

It is worth mentioning that this was the cheapest way to have second-order approximation as the calculations with different meshes were mandatory because of the bifurcation nature of the problem. In turn using a $O(h)$ scheme for a given set of mesh parameters was much more efficient in the sense of stability and required a fewer number of iterations. So, when dealing in the next section with the KSV equation we shall

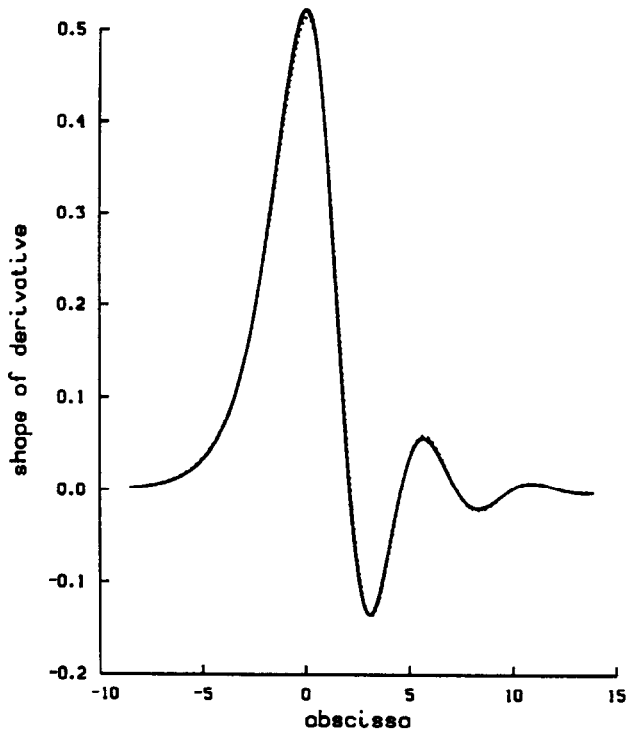

Figure 2. The influence of the mesh size N on the calculated shape of the solitary wave: One extreme case solid line (——) $N = 401$; the other values correspond to $N = 801$, $N = 1601$, $N = 3201$, and the broken line (----) $N = 6401$. They are nearly indistinguishable.

present results obtained after applying Richardson's extrapolation, i.e., results with accuracy $O(h^2)$.

Before closing this section let us emphasize that contrary to earlier statements in the literature[8,12,18] the spectrum is discrete and consists only of one value.

KSV equation—the case of negative δ

After clarifying the issue regarding the existence of a solitary wave in the KS equation we come back to the problem of finding the solitary waves for the KSV equation (3). The two cases, $\delta < 0$ (negative) and $\delta > 0$ (positive), are expected to exhibit quite different features because of the fact that the solution for u is in fact a kink (when a homoclinics is sought for v), i.e., the asymptotic behavior of both infinities is strongly asymmetrical with an increase of δ in either the positive or negative direction.

Guided by the notion that for small but negative δ the general appearance of the kink for u (or the hump for v)

must be similar to KS, we can conclude that the scale of the solitary wave is not drastically changed. Thus we can smoothly proceed from the pure KS case to the KSV equation. For this reason we start with the case of negative δ, when the corresponding nonlinear term in equation (3) plays a stabilizing role.

There is no need to give again a description of the minimization procedure already described. Suffice it to add that some preliminary work with the algorithm must be performed for each δ in order to locate roughly the interval for the minimum of c. Note that in the preliminary calculations connected with the rough location of the minimum we found also the optimal L and NS for the given value of δ. The value of the functional was always of the order 5.10^{-8}. Results were obtained for $\delta = -0.1, \ldots, -0.7, -0.75, -0.8, -0.85$.

The most important conclusion from the extensive set of calculations is that the solitary wave shape changes when approaching the limit $\delta = -0.87$, and for the last value even the wave forerunning front disappears. The gradual evolution of the solution with δ is shown in *Figures 3* and *4*. Correspondingly, *Figures 3a* and *4a* present the *kink*, which is the actual solution (an integral of the solitary wave of *Figures 3b* and *4b*). The reader should not be confused by the fact that in Ref. 8 an apparently similar disappearance of the forerunner with increasing δ takes place. However, δ is the coefficient of the third derivative in space, and hence it reflects different physical mechanisms.

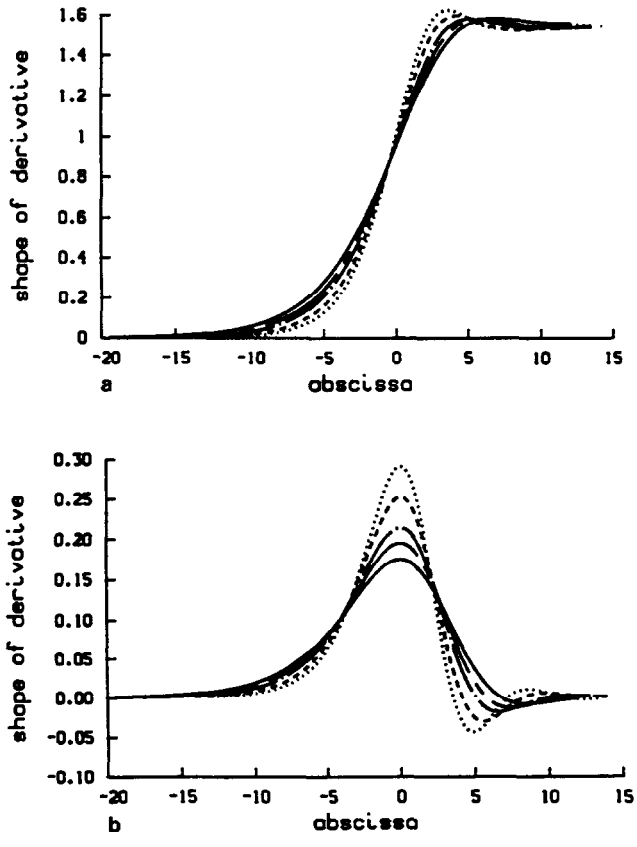

Figure 3. The localized solution for *negative* values of δ: (a) kink shape, (b) its derivative. (····) $\delta = 0$; (----) $\delta = -0.1$; (-●-) $\delta = -0.2$; (---) $\delta = -0.3$; (——) $\delta = -0.4$.

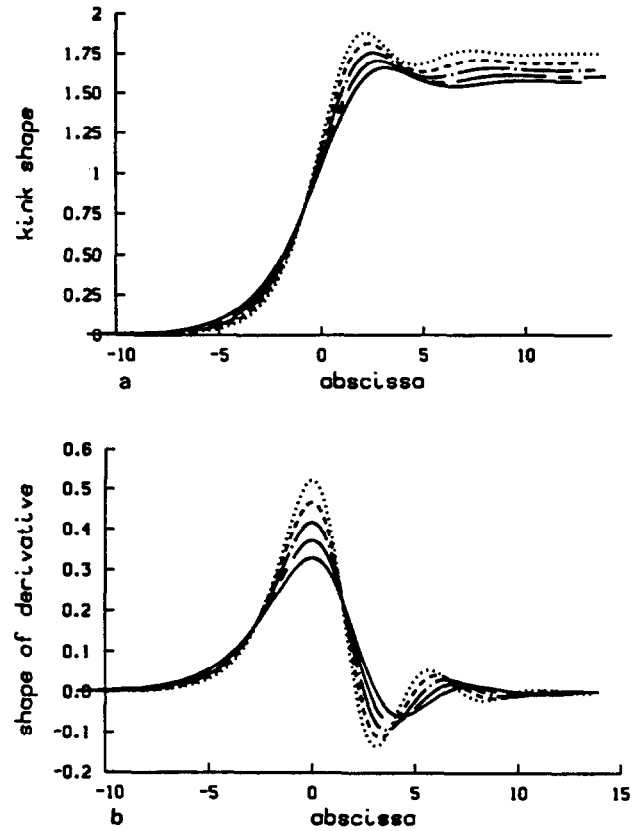

Figure 4. The localized solution for *negative* values of δ: (a) kink shape, (b) its derivative. (····) $\delta = -0.5$; (----) $\delta = -0.6$; (-●-) $\delta = -0.7$; (---) $\delta = -0.75$; (——) $\delta = -0.8$.

KSV equation—the case of positive δ

Let us turn now to the case with positive δ, when the corresponding nonlinear term in equation (3) contributes to destabilizing the solution. It can be shown that in this case the linearized equation contains the coefficient $(1 + \delta u_{+\infty})$ for $\xi \gg 1$. This coefficient governs the properties of the forerunner. The latter decays faster now with $\xi \to \infty$, but at the same time its wavelength becomes shorter, and this makes the numerical problem even harder because of the increased gradients of the solution. It goes without saying that the value of L and the ratio NS/N were being adjusted *a posteriori* with increasing δ. There is another difficulty to tackle for positive δ, and it is again connected with the coefficient $(1 + \delta u_{+\infty})$ because it is a functional of the flow, and as a result a positive feedback occurs in the iteration process, which can lead to instability. This instability is easily overcome by means of relaxation.

In *Figures 5a* and *5b* are presented respectively the results for v and u in the interval $\delta \in [0, 0.8]$. The above-discussed tendency of the solution to shorten its support in the region of positive values of the argument is clearly seen. In addition the *celerity* increases with

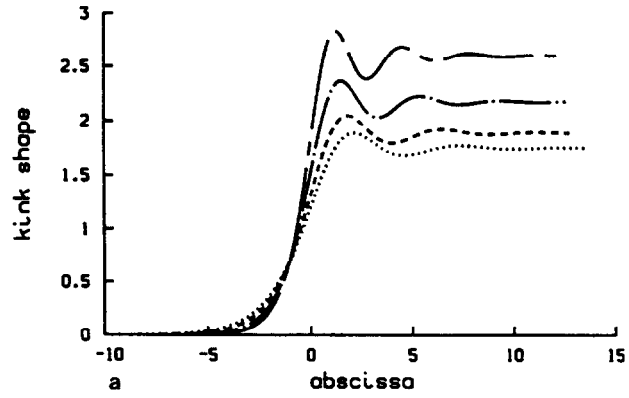

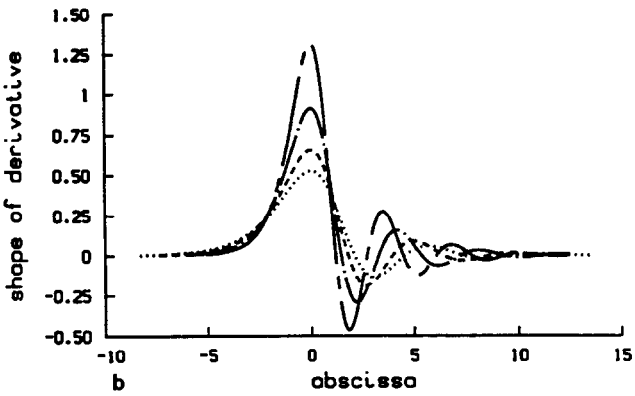

Figure 5. The localized solution for *positive* values of δ: (a) kink shape, (b) its derivative. (····) $\delta = 0$; (----) $\delta = 0.2$; (-●-) $\delta = 0.5$; (—·—) $\delta = 0.8$.

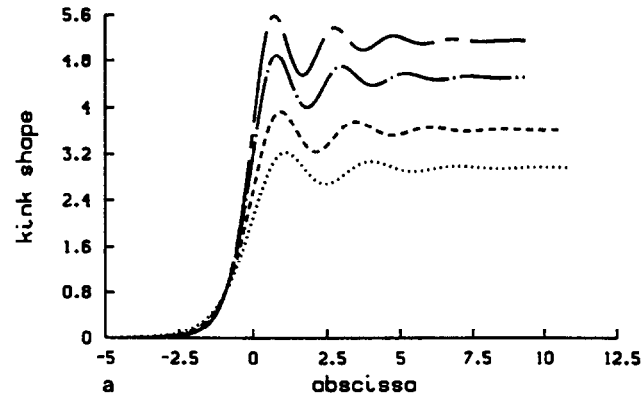

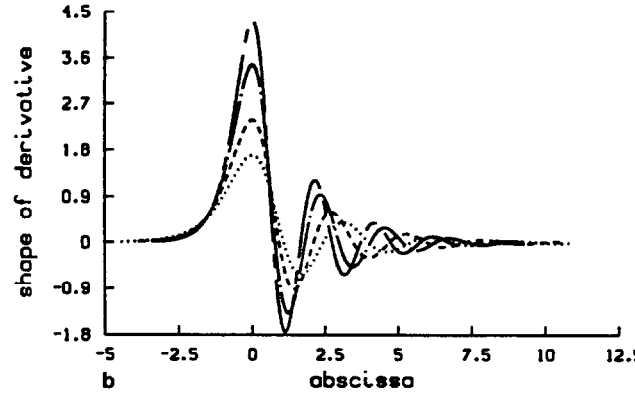

Figure 6. The localized solution for *positive* values of δ: (a) kink shape, (b) its derivative. (····) $\delta = 1.0$; (----) $\delta = 1.2$; (-●-) $\delta = 1.4$; (—·—) $\delta = 1.5$.

the increase of δ, i.e., the solitary wave becomes swifter. This means that the value of c for a smaller δ is already not as convenient an approximation when moving to higher δ, and therefore a considerable number of numerical experiments need to be performed to localize the minimum of $f(c)$ before proceeding with the golden section minimization procedure.

The above-described tendency is even more conspicuous in *Figures 6a* and *6b*, where the range of the main governing parameter is $\delta \in [1.0, 1.5]$.

The dependence of c and δ is summarized in *Figure 7*. Unfortunately, it is not obvious what kind of analytic expression for the correlation between c and δ is to be expected. What is obvious is that c increases faster than an exponent for $\delta > 0$ and decreases slower than an exponent for $\delta < 0$.

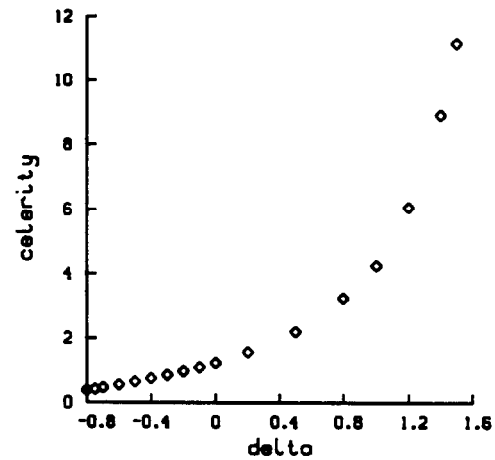

Figure 7. Dependence of the celerity "c" of the localized solution/solitary wave on the parameter δ.

Conclusion

In this paper the problem of *localized* solutions (solitary waves) to a generalization of the Kuramoto–Sivashinky equation (called the KSV equation) is treated numerically by means of a method of variational imbedding. The convergence of the difference solution to the solution of the differential equation is proved by means of mandatory numerical experiments with different mesh sizes, "actual infinity", etc. The accuracy of the solution is improved by means of Richardson extrapolation.

First, the technique is applied to the problem of homoclinic solutions of the original KS equation. It appears that a single-hump homoclinics exists only for one value of the celerity $c^* = 1.216$, which is in perfect agreement with the results of other authors. Then the

kink solutions of the KSV equation are obtained for different values of an additional governing parameter δ (note that for $\delta = 0$ the spatial derivative of the kink solution of the KSV equation coincides with the homoclinics of the KS equation). For each δ a single eigenvalue c^* for the celerity is obtained. The correlation between δ and c^* is also graphically presented.

Our interest in the nonlinear term with the coefficient δ in equation (1) is because this term has some physical content that changes with its sign! Indeed it can change sign according to the *effective* gravity level, and thus equation (1) accounts for both ground and space (microgravity) conditions. When $\delta < 0$ (negative) this term plays a stabilizing role whereas if $\delta > 0$ (positive) it tends to destabilize the surface. This is confirmed by our numerical results. They show that for negative δ the wavy forerunner gradually disappears while in the opposite case of positive δ the solitary wave becomes swifter, and the forerunner becomes sharper. For a rigorous discussion of the initial value problem and asymptotic low dimensional behavior of equation (1), see Ref. 19.

Acknowledgment

The first author wishes to express his appreciation of the hospitality offered by Dra. R. Díaz-Pabón at the Spanish Meteorological Institute where he held a sabbatical position sponsored by the DGCYT from the Spanish Ministry of Education and Science. He also acknowledges the hospitality of Prof. G. S. Maugin at the University Paris-VI where part of this work was carried out. This research has been supported by Grant 1052 of the Bulgarian Ministry of Science and Higher Education and by CICYT (Spain) under Grants PB 86-651 and PB-90-264.

References

1 Koschmieder, E. L. *Adv. Chem. Phys.* 1974, **26,** 177
2 Velarde, M. G. and Normand, C. *Sci. Am.* 1980, **243(7), 92**
3 The role and relevance of the Marangoni effect in science and engineering is extensively described in several chapters of *Physicochemical Hydrodynamics. Interfacial Phenomena*, ed. M. G. Velarde, Plenum Press, NY, 1988
4 Davis, S. H. and Homsy, G. M. *J. Fluid Mech.* 1980, **98,** 527
5 Castillo, J. L., Garcia Ybarra, P. L., and Velarde, M. G. Thermohydrodynamic instabilities. *Synergetics and Dynamic Instabilities*, ed. G. Caglioti, H. Haken, and L. A. Lugiato, North Holland, Amsterdam, 1988
6 Hyman, J. M. and Nicolaenko, B. Coherence and chaos in the Kuramoto–Velarde equation. *Partial Differential Equations*, ed. M. Crandall, Academic Press, NY, 1987
7 Hyman, J. M. and Nicolaenko, B. *Physica* 1986, **18D,** 113
8 Kawahara, T. and Toh, S. *Phys. Fluids* 1988, **31,** 2103
9 Garazo, A. N. and Velarde, M. G. *Phys. Fluids* 1991, **A3,** 2295
10 Kakutani, T. and Kawahara, T. *J. Phys. Soc. (Japan)* 1970, **29,** 1068
11 Christov, C. I. A method for identifying homoclinic trajectories. *Proceedings of the 14th Spring Conference, Union of Bulgarian Mathematicians*. Sunny Beach, Bulgaria, 1985, pp. 571–577
12 Christov, C. I. and Nartov, V. P. The use of method of variational imbedding for calculating solitons in falling-liquid-film flow. *Proceedings of the Conference Anniversary of Academician L. Tchakalov*. Samokov, Bulgaria, 1986, pp. 135–142 (in Russian)
13 Pumir, A., Manneville, P., and Pomeau, Y. *J. Fluid Mech.* 1983, **135,** 27
14 Shkadov, V. Ya. *Izv. Akad. Nauk SSSR, Mechanika Zhidkosti i Gasa* 1977, **1,** 63–66 (in Russian)
15 Forsythe, G. E., Malcom, M. A., and Moler, C. B. *Computer Methods for Mathematical Computations*. Prentice Hall, Englewood Cliffs, NJ, 1977
16 Tzvelodub, O. Yn. *Izr. Akad. Nauk SSSR, Mechanika Zhidkosti i Gasa* 1980, **4,** 142 (in Russian)
17 Christov, C. I. in *Lecture Notes in Fluid Physics*, ed. M. G. Velarde, World Scientific, London, to be published
18 Chang, H.-C. *Phys. Fluids* 1986, **29,** 3142
19 Rodriguez-Bernal, A. *Nonlinear Analysis T.M.A.* 1992, **19,** 643